Flow patterns and sediment deposition in rectangular shallow reservoirs

M. Dufresne[1]*, B. Dewals[1], S. Erpicum[1], P. Archambeau[1] and M. Pirotton[1]

[1] University of Liège (ULg), ArGEnCo department, Hydraulics in Environmental and Civil Engineering (HECE), Chemin des chevreuils, 1, bât B52/3, étage +1, 4000 Liège, Belgium
(E-mail: b.dewals@ulg.ac.be)
* (Present address) National school for water and environmental engineering (ENGEES), Fluid and solid mechanics institute (IMFS), adress: IMFS, 2 rue Boussingault 67000 Strasbourg, France (E-mail: matthieu.dufresne@engees.unistra.fr)

Keywords
flow patterns; rectangular shallow reservoirs; sediment deposition.

Abstract
This work involves the experimental investigation of flow patterns, preferential regions of deposition and trapping efficiency in rectangular shallow reservoirs. The main flow patterns that can be encountered in rectangular shallow reservoirs are described: symmetrical flows without any reattachment point (S0), asymmetrical flows with one reattachment point (A1), and asymmetrical flows with two reattachment points (A2). The influence of geometrical and hydraulic parameters on reattachment lengths is intensively investigated. A shape parameter is introduced to classify symmetrical and asymmetrical flows. For each flow pattern, the preferential regions of deposition are studied. To conclude, a number of practical recommendations are given. Reservoirs with a shape parameter lower than 6.2 limit sediment deposition. Reservoirs with a shape parameter greater than 6.8 are favourable for sediment deposition. Finally, perspectives for maximizing and minimizing deposition are given, respectively by exploiting the great trapping potential of the flow pattern A1 and the poor trapping potential of the flow pattern S0.

Introduction
Reservoirs are commonly used for stormwater management. Because of generally quiescent conditions, these works are conducive to the settling of particles. Therefore, reservoirs must be carefully designed according to the role they will play: sedimentation must be maximized in settling basins whereas one generally wants to minimize it in storage facilities. Inappropriate design may result, respectively, in a poor quality of the downstream watercourses (high concentrations of suspended load in overflows) and in excessive operating costs (frequent removal of sediments).

Whereas design methods generally provide only the volume of the reservoir, no definitive rule is available for determining the shape and the dimensions of the structure. Indeed, the prediction of deposition as a function of the geometry of the reservoir, the hydraulic conditions and the sediment characteristics is still a great challenge. While empirical and semi-empirical methods have been developed for the last sixty years to determine the amount of deposits (see for example Garde *et al*. 1990, Ranga Raju *et al*. 1999; see also Kowalski *et al*. 1999 for combined sewer detention tanks, Luyckx *et al*. 1999 for high side weir

overflows), they cannot determine their spatial distribution, which is required to well define the sediment removal strategy. To get this information, the knowledge of the flow pattern is a prerequisite. It is also questionable whether the relative imprecision of these methods is not because they express the trapping efficiency of the reservoir without taking into account the flow pattern. Indeed, these methods generally use mean hydraulic variables (such as the mean transversal velocity) whereas complex flows can take place even in simple geometries.

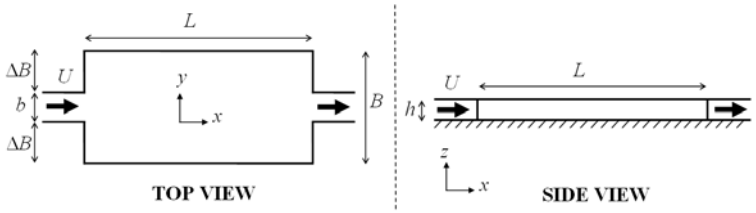

Fig. 1. Schemes of a rectangular shallow reservoir.

Rather than considering a complex geometry that would be a special case, this study focuses on a very simple geometry: the rectangular shallow reservoirs. As illustrated in figure 1, the geometry consists of an upstream expansion and a downstream contraction, which may lead – despite the symmetry – to asymmetrical flow pattern (Kantoush *et al*. 2008).

The aim of the present study is to classify the flow patterns that can be encountered in rectangular shallow reservoirs, to determine the influence of the flow pattern on sediment deposition and to give practical recommendations.

Bibliographic review

Flow

If we assume that the flow is governed by the length of the reservoir (L), the lateral expansion (ΔB), the breadth of the inlet and outlet channels (b), the water depth (h), the mean depth-averaged velocity (U), the bed shear stress (τ), the water density (ρ), the water viscosity (μ) and the gravitational acceleration (g) – which are a set of nine variables involving time, mass and length unities – dimensional analysis principles can reduce the problem to six dimensionless parameters (Langhaar 1951). For example, one can choose a lateral expansion ratio ($\Delta B/b$), a dimensionless length ($L/\Delta B$), a dimensionless water depth ($h/\Delta B$), a Froude number ($U/(gh)^{0.5}$), a Reynolds number ($4\rho Uh/\mu$), and a bed friction number ($c_f \Delta B/2h$). Here, c_f is the bed friction coefficient ($2\tau/\rho U^2$); it can be estimated using a 'Colebrook' formula (see for example Henderson 1966, p. 95).

For "infinitively" long reservoirs (there was no contraction downstream), Abbott and Kline (1962) showed that the recirculation zones in each side of the expansion were equal in length for lateral expansion ratio lower than 0.25 and different for lateral expansion ratio greater than 0.25.

Kantoush (2008) showed that decreasing the dimensionless length of a rectangular shallow reservoir from 3.2 to 2.7 induced a transition from an asymmetrical flow with one reattachment point (also called "stagnation" or "separation" point in the literature) to a symmetrical flow without any reattachment point.

When decreasing the dimensionless water depth (but increasing the Froude number in the same time), Kantoush (2008) showed that the flow became unsteady ("meandering jet"). This

behavior is similar to the observations of Giger *et al*. (1991) about plane turbulent jets in shallow water and those of Chen and Jirka (1995) about the turbulent wakes generated by two-dimensional bodies in shallow water.

To our knowledge, the influence of the Froude number on the flow pattern has never been intensively studied in isolation. Only Kantoush (2008) carried out one experiment, decreasing the Froude number from 0.10 to 0.05 (keeping the same dimensionless water depth); his results did not highlight any significant influence of this parameter on the flow pattern.

Abbott and Kline (1962) claimed that the flow pattern was not sensitive to the Reynolds number, provided the flow was fully turbulent before the expansion. Casarsa and Giannattasio (2008) carried out PIV (particle image velocimetry) measurements in order to check this behavior and showed that the influence of this dimensionless parameter on the shorter reattachment length was not completely negligible (a few percents). It must be noted that the present study only focuses on large Reynolds numbers; transitions from symmetrical to asymmetrical flows that can be encountered at small and moderate Reynolds numbers are not considered (see for example Cherdron *et al*. 1978, Fearn *et al*. 1990, Maurel *et al*. 1996).

Friction effects have been intensively investigated for shallow recirculating flows over single lateral expansions (Babarutsi *et al*. 1989, Babarutsi and Chu 1991, Chu *et al*. 2004). These studies highlighted two asymptotic behaviors, depending on the bed friction number: for small values of this dimensionless parameter, the reattachment length is only dependent on the horizontal geometry; for large values, the reattachment length is only dependent on the friction length scale (defined as the ratio of the water depth to the bed friction coefficient).

This study focuses on geometrical (lateral expansion ratio, dimensionless length) and hydraulic parameters (dimensionless water depth, Froude number) under conditions such that the Reynolds number and the bed friction number are respectively large enough and small enough not to influence the flow pattern.

Sediment deposition

Saul and Ellis (1992) highlighted that complex flow patterns could take place in rectangular tanks and that the flow pattern governed the sediment transport processes. Stovin and Saul (1994) carried out experiments in a rectangular chamber with particles of crushed olive stone. The flow field was characterised by a large clockwise circulation and a small counter clockwise circulation in the upstream left corner of the tank (asymmetrical flow pattern). Deposits were located in three preferential regions: in both upstream corners of the tank and in the core of the large circulation zone. Varying the inflow velocity, Stovin and Saul (1996) proposed a linear relationship between the percentage of the bed that is covered by deposits and the trapping efficiency.

Kantoush (2008) used crushed walnut shells in order to study morphological evolution in rectangular shallow reservoirs. Nevertheless, the flow pattern was not steady during sediment tests, probably because of the large amount of deposits near the inlet of the reservoir.

A number of experimental studies have been conducted in more complex geometries. Stovin (1996) investigated some effects of a V-shaped benching and the length to breadth ratio on sediment distribution. A study performed in a three-dimensional geometry (the inlet pipe was located near the bottom of the upstream face of the tank) highlighted a transition from

asymmetrical to quasi-symmetrical flow and deposit patterns when increasing the water depth (Dufresne 2008).

Experimental investigation

Experimental device

The experiments were carried out at the laboratory of engineering hydraulics of the University of Liège, Belgium. The experimental device, as illustrated in figure 2, consists of a 10.40 m long and 0.985 m wide glass channel in which blocks can be arranged to build different geometries of rectangular reservoirs. The base of the flume is horizontal.

The flow enters the channel from a stilling basin through a porous screen in order to prevent fluctuations in water level and make the velocity field uniform. The flow is then contracted to the desired breadth of the inlet channel (b) in a converging section with circular shape; the inlet section of the reservoir (with straight parallel walls) is 2.00 m long. At the entrance of the reservoir, the flow suddenly expands to the breadth of the reservoir (B). At the exit of the reservoir, the flow suddenly contracts to the outlet channel breadth (b). The outlet channel is 1.00 m long; its downstream boundary corresponds to a gate (to control the water level) and a waterfall. All the surfaces are made of glass, except the two parallel walls of the inlet and outlet channels (PVC) and the converging section (metallic sheets).

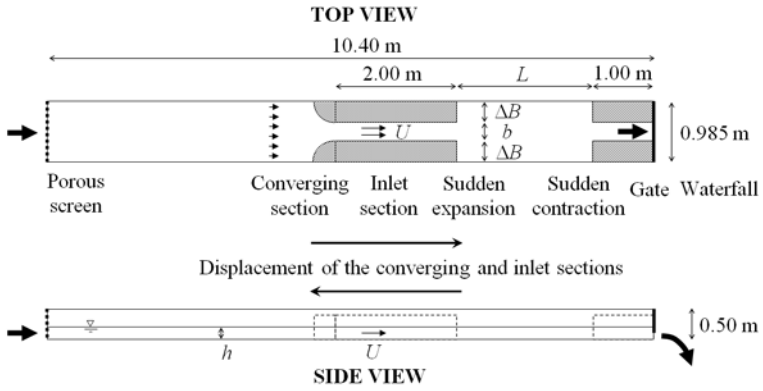

Fig. 2. Sketch of the experimental device.

In order to vary the lateral expansion ratio, two different sizes of blocks were used (ΔB = 0.250 and 0.350 m) and an additional glass wall was placed along one wall of the flume for part of the experiments in order to reduce the breadth of the reservoir (from 0.985 to 0.780 m). The length was varied up to 7.000 m.

The flow rate was measured with an electromagnetic flowmeter upstream of the flume; it was also measured with a triangular weir in the water collection channel downstream of the waterfall in order to enhance accuracy on small values. Water depth in the reservoir was measured with a level meter in the middle of the breadth 0.10 m downstream of the entrance of the reservoir and 0.10 m upstream of the exit of the reservoir (the maximum difference between the two values was 0.002 m). The range of flow discharge was between 1.6 and 79 l/s.

The water temperature was between 18 and 20 °C, depending on the experiment. In order to check the reproducibility, all the experiments for which the flow was steady were repeated. The tolerance in the dimensions of the reservoir was 0.005 m. The uncertainty is about 0.002

m in the water depth (level meter) and about 0.01 m/s in the velocity, except for low water depths ($h \approx 0.050$ m) and narrow inlet channel ($b = 0.080$ m) for which it is up to 0.04 m/s.

Flow tests

Visual investigations employing dye injections disclosed the flow pattern: symmetry or asymmetry, number of circulation zones, approximate locations of reattachment points. Once the reattachment length had been roughly estimated, we precisely measured it using an original, simple and robust protocol: the method consists in injecting drops of dye at various x-positions against the wall near the stagnation point (at $z = 0.04$ m above the bed) in order to determinate the proportion of negative velocities (from downstream to upstream). Using the proportions measured for different abscissas, we calculated a 95% confidence interval of the median reattachment length (measurement uncertainty) and extracted the natural variability (unsteadiness of the flow despite steady boundary conditions). A complete description of the protocol and the experimental data (forty geometrical and hydraulic conditions) can be found in a previous article (Dufresne *et al*. 2010a).

Sediment tests

Granular plastic (Styrolux 656 C) was chosen as the model sediment. The particles are elliptical cylinders with a density of 1,020 kg/m^3 (given by the producer BASF) and a characteristic grain size of 2.4 mm. This type of sediment was selected in order to simulate the coarsest fraction of sediments typically found in stromwater ($d > d_{90}$), which is the fraction most prone to deposition. Indeed, the application of the Shields similarity and the grain Reynolds number similarity leads to a prototype particle size of ≈ 0.6 mm and a particle density of $\approx 2.2 \times 10^3$ kg/m^3 for a geometric scaling factor of 15 (Luyckx *et al*. 1999). In order to avoid flocculation, the plastic sediment had been wet prior to experiment. It was input into the inflow 2.00 m upstream of the entrance of the reservoir. The injection consisted in discrete batches of 80 g (dry mass) over 10 second time intervals. The total period of injection was 10 minutes for each experiment. The inflow concentration was 0.50 g/L. Based on uncertainties in discharge, sediment mass and time period, the uncertainty in the inflow concentration is about 0.02 g/L. Using a net, particles were collected in the waterfall downstream of the reservoir in three time periods: between 2 and 4 minutes after the beginning of the injection, between 5 and 7 minutes, and between 8 and 10 minutes. Each sample was dried and weighted, so that the mean outflow concentration could be calculated for the three time intervals. The trapping efficiency, η, was calculated for each period using equation 1 (some values were rejected since equilibrium between inlet and outlet was not reached). Here, c_{in} = inflow concentration; c_{out} = outflow concentration. The uncertainty in the outflow concentration is between 0.005 and 0.020 g/L (depending on the outflow concentration), which leads to an absolute uncertainty in the efficiency of 0.10 – 0.15.

$$\eta = \frac{c_{in} - c_{out}}{c_{in}} \quad (1)$$

Only three experimental conditions were investigated for sediment tests (one for each main flow pattern); all the experimental data are reported in a previous article (Dufresne *et al*. 2010b).

Classification of flow patterns

Description of the main flow patterns

For short reservoirs, the flow presents a symmetrical behavior without any reattachment point ("S0" in figure 3). The jet goes in a straight way from the entrance to the exit of the reservoir; two symmetrical circulation zones take place.

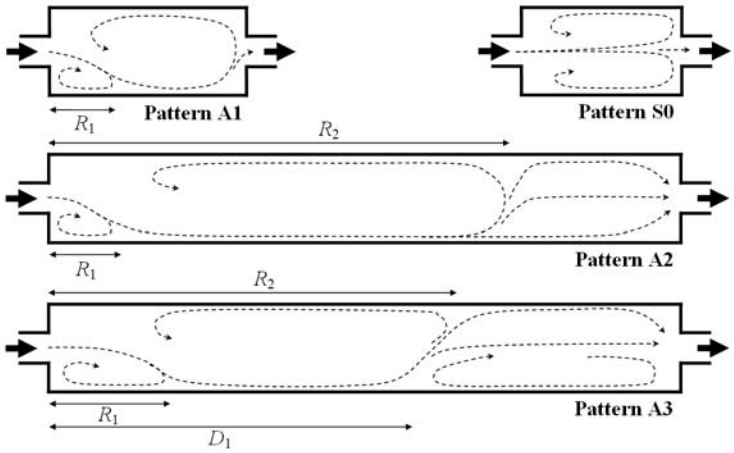

Fig. 3. Schemes of the main flow patterns.

Symmetry disappears when increasing the dimensionless length ("A1" in figure 3). The jet is deflected on one side of the reservoir (right or left, depending on the test). It reattaches the wall after a distance denoted by "R1" in figure 3, which leads to the formation of a large circulation zone. A smaller circulation zone takes place upstream of the reattachment point.
For intermediate dimensionless lengths, we observed that the flow did not stabilize in spite of steady boundary conditions: it fluctuated between a symmetrical (S0) and an asymmetrical behavior (A1). The fluctuations between these two patterns were not periodic and seemed to be completely random. This type of flow is reported as "A1/S0" below.

When increasing again the dimensionless length, the flow still remains asymmetrical ("A2" in figure 3). As for the pattern A1, the flow reattaches on one side of the reservoir after a distance R_1 but also on the opposite wall after a distance R_2. In this situation, the flow is fully reattached in the downstream zone of the basin.

Figure 3 illustrates the "mean" flow patterns; analysis of flow test results showed that, despite steady boundary conditions, the reattachment lengths presented a relatively high natural variability, especially the longer one (Dufresne *et al*. 2010a). This variability will undoubtedly have consequences on deposits.

Influence of the hydraulic dimensionless parameters

The influence of the hydraulic dimensionless parameters was intensively studied for "long" reservoirs (dimensionless lengths: 20.0, 28.0); this corresponds to the flow pattern A2. Regarding the dimensionless water depth (investigated in the range 0.10 – 1.60), the main result is that increasing this parameter induces a decrease of the median value of the shorter reattachment length (R_1) until it reaches a minimum level (for "high" water depths). Decreasing the dimensionless water depth (below ≈ 0.2) also induces a third recirculation zone in the downstream zone of the reservoir (pattern A3). Regarding the Froude number (investigated in the range 0.05 – 0.40), the main result is that increase of this parameter is also responsible for a decrease of the median value of the shorter reattachment length.

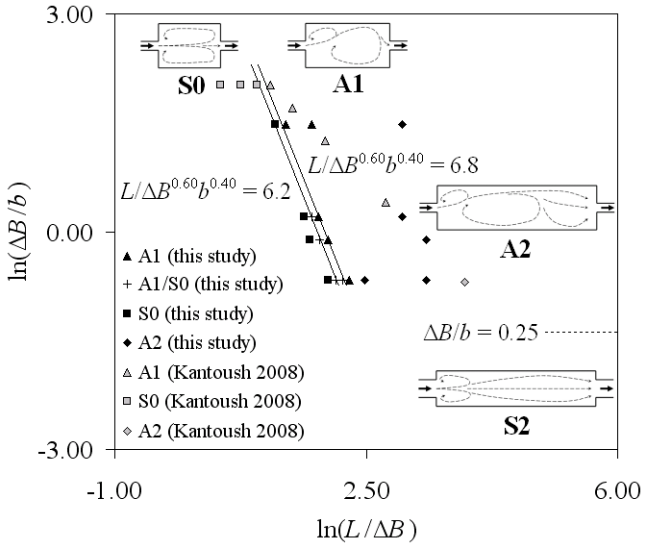

Fig. 4. Classification diagram of the flow patterns for "high" water depths and a Froude number of 0.20.

Influence of the geometrical dimensionless parameters

Here, we only consider a Froude number of 0.20 and a dimensionless water depth in the range 0.57 – 0.80, which corresponds to "high" water depths. Figure 4 illustrates all the flow patterns that we observed when varying the geometry in these conditions. The x-coordinate and the *y*-coordinate of this figure are respectively the natural logarithm of the dimensionless length and the natural logarithm of the lateral expansion ratio. This figure identifies a transition criterion between symmetrical and asymmetrical flows as a combination of the dimensionless length and the lateral expansion ratio (equation 2) rather than only the dimensionless length. When this "shape parameter" is lower than ≈ 6.2, the flow is symmetrical (S0); when it is greater than ≈ 6.8, the flow is asymmetrical (A1 or A2, depending on the length of the reservoir). For intermediate values, unstable flows may take place (A1/S0).

$$\text{Shape parameter} = \left(\frac{L}{\Delta B}\right)\left(\frac{\Delta B}{b}\right)^{0.40} = \frac{L}{\Delta B^{0.60} b^{0.40}} \qquad (2)$$

Even if they have been obtained for smaller dimensionless water depths (in the range 0.11 – 0.60) and a smaller Froude number (0.10), the results of Kantoush (2008) are also consistent with these critical values (see figure 4).

For "long" reservoirs (A2), the median value of the shorter reattachment length can be approximated by equation 3. Near the transition between patterns S0 and A1 (for the "last" asymmetrical flow), equation 4 was found to be a good approximation.

$$R_1 \approx 3.43 \Delta B^{0.75} b^{0.25} \qquad (3)$$

$$R_1 \approx 3.27 \Delta B^{0.60} b^{0.40} \qquad (4)$$

Using very limited results (two measurements) and assuming the same type of power law, the median value of the longer reattachment length can be roughly approximated by equation 5.

$$R_2 \approx 15.9 \Delta B^{1.7} b^{-0.7} \quad (5)$$

Influence of the flow pattern on sediment deposition

Spatial distribution

Figure 5 illustrates the preferential regions of deposition after 10 minutes of sediment input for the three experimental conditions we investigated (a clear pattern of deposition was observed after 4 – 5 minutes for all the sediment tests); two tests were carried out for each experimental condition (grey zones and dotted lines). For these experiments, the dimensionless length was 5.1, 5.7 and 20.0; the lateral expansion ratio, 1.23; the dimensionless water depth, between 0.56 and 0.59; the Froude number, between 0.19 and 0.21; the Reynolds number between 210,000 and 228,000; the bed friction number, around 0.003 (with ΔB = 0.350 m).

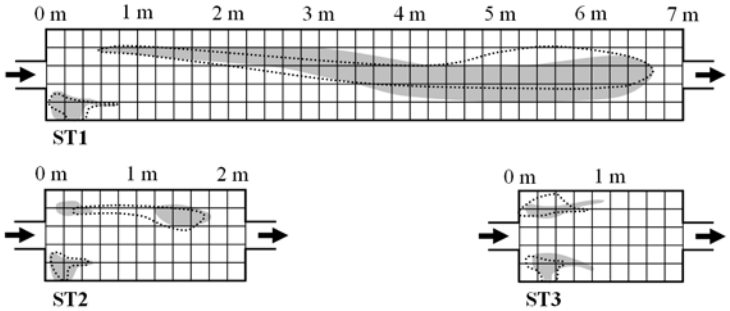

Fig. 5. Deposit patterns (two tests for each experimental condition).

From this figure, it can be concluded that the location of the deposits is clearly a function of the flow pattern. For the flow pattern S0, the deposit pattern is quasi-symmetrical (see "ST3"). Deposition takes place in each inlet corners. The shape of the downstream part of these zones is elongated and corresponds to deposits regularly eroded (wake zone of the flow).

For the flow pattern A1, the deposit pattern is asymmetrical (see "ST2"). Three regions of deposition take place on the bed: the two inlet corners and the core of the large circulation zone. Despite its relatively small area, the region of deposition in the core of the large circulation zone contains the largest amount of deposits; in this zone, the deposits were regularly eroded due to the relative unsteadiness of the flow, but they remained captured in the circulation current and escaped only by intermittent "bursts".

For the flow pattern A2, the deposit pattern is still asymmetrical (see "ST1"). A first region of deposition takes place in one inlet corner; a second one, in the downstream zone of the reservoir (its length was about 6.0 m).

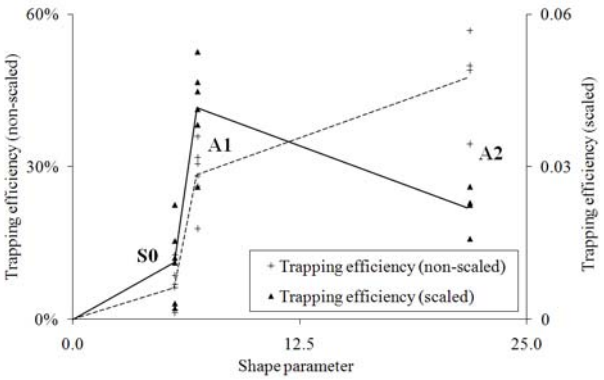

Fig. 6. Trapping efficiency as a function of the shape parameter.

Trapping efficiency

Figure 6 illustrates the trapping efficiency as a function of the shape parameter. Even if the values are relatively scattered for a given shape parameter (because of the measurement uncertainty and also the natural variability), the general tendency is unambiguous: the transition between symmetrical and asymmetrical flows is responsible for an abrupt increase in the efficiency curve (see the dotted line for the general tendency). Indeed, for a shape parameter of 5.6 (pattern S0), the efficiency is in the range 0% – 20% (mean value: 6%); for 6.8 (pattern A1), the efficiency is the range 10% – 40% (mean value: 28%). The efficiency still increases when increasing the shape parameter to 21.7 (pattern A2): $\eta = 30\% - 60\%$ (mean value: 48%); nevertheless, the slope of the tendency between 6.8 and 21.7 is much lower than between 5.6 and 6.8. In order to take into account the length of the reservoir, the trapping efficiency has been scaled with the shape parameter, as written in equation 6.

$$\eta_{scaled} = \frac{\eta}{L \Big/ \Delta B^{0.60} b^{0.40}} \quad (6)$$

As illustrated in figure 6 (solid line), the tendency of the scaled efficiency exhibits a maximum for the flow pattern A1, which highlights a great trapping "potential" of this flow pattern. This can be explained by the fact that the deposits obtained for the flow pattern A1 were concentrated in the core of the circulation zone whereas they were dispersed over an approximate length of 6.0 m for the flow pattern A2 (see figure 5). In other words, the flow pattern A1 maximizes the deposition compared to the length of the reservoir. This figure also highlights the poor trapping potential of the flow pattern S0.

Conclusions

(1) The main flow patterns that can be encountered in rectangular shallow reservoirs were described: symmetrical flows without any reattachment point (S0), asymmetrical flows with one reattachment point (A1), and asymmetrical flows with two reattachment points (A2). The influence of the geometrical and hydraulic parameters was described in details. A shape parameter ($L/\Delta B^{0.60} b^{0.40}$) was introduced to classify symmetrical and asymmetrical flows.

(2) For each flow pattern, the preferential regions of deposition were described. This showed that the transition between symmetrical and asymmetrical flows was responsible for an abrupt increase of the trapping efficiency. Finally, the great trapping potential of the flow pattern A1 and the poor trapping potential of the flow pattern S0 were highlighted compared to the flow pattern A2.

(3) Despite the limited experimental conditions that have been investigated for the sediment tests, a number of practical guidelines can be given:

- Reservoirs with a shape parameter lower than 6.2 limit sediment deposition.
- Reservoirs with a shape parameter greater than 6.8 are favourable for sediment deposition.
- The great trapping potential of the flow pattern A1 can be exploited by partitioning a long reservoir in several facilities in order to maximize the amount of deposits. For example, the trapping efficiency of the 7.000 m long reservoir is ≈ 48% (mean value); three successive 2.200 m long reservoirs ($\eta \approx 28\%$ for each one; total length = 6.600 m) would lead to a global efficiency of ≈ 63%, which is about 30% greater.
- The poor trapping potential of the flow pattern S0 can be exploited by partitioning a long reservoir in several shorter facilities in order to minimize the amount of deposits. Four successive 1.800 m long reservoirs ($\eta \approx 6\%$ for each one; total length = 7.200 m) would lead to a global efficiency of ≈ 22%, which is about half the efficiency of the 7.000 m long reservoir (≈ 48%).

(4) Regarding the flow, further work is required to assess the influence of the Froude number and the dimensionless water depth near the transition between symmetrical and asymmetrical flows. Additional experiments are also needed to better describe the longer reattachment length (R_2).

(5) Since we carried out only a small number of sediment tests, further work is required to generalize the conclusions to broader conditions (geometrical parameters, hydraulic parameters and sediment characteristics). We believe that it is necessary to proceed by steps: each dimensionless parameter should be integrated gradually in order to define a physically based relationship for the trapping efficiency.

Acknowledgments

We acknowledge Alain Dewart, Didier Lallemand, Maurice Salme and Dieudonné Stouvenakers for the building of the experimental device. We also acknowledge the University of Liège for the allocation of a postdoctoral fellowship to the first author.

References

Abbott, D.E. and Kline, S.J. (1962) Experimental investigation of subsonic turbulent flow over single and double backward facing steps. *Journal of Basic Engineering*, 317-325.

Ashley, R.M., Bertrand-Krajewski, J.L., Hvitved-Jacobsen, T. and Verbanck, M. (2004) Solids in sewers: characteristics, effects and control of sewer solids and associated pollutants. IWA Publishing.Babarutsi, S. and Chu, V.H. (1991) Dye-concentration distribution in shallow recirculating flows. *Journal of Hydraulic Engineering*, **117**(5), 643-659.

Babarutsi, S., Ganoulis, J. and Chu, V.H. (1989) Experimental investigation of shallow recirculating flows. *Journal of Hydraulic Engineering*, **115** (7), 906-924.

Casarsa, L. and Giannattasio, P. (2008) Three-dimensional features of the turbulent flow through a planar sudden expansion. *Physics of Fluids*, **20**, 5103:1-15.

Chen, D. and Jirka, G.H. (1995) Experimental study of plane turbulent wakes in a shallow water layer. *Fluid Dynamics Research*, **16** (1), 11-41.

Cherdron, W., Durst, F. and Whitelaw, J.H. (1978) Asymmetric flows and instabilities in symmetric ducts with sudden expansions. *Journal of Fluid Mechanics*, **84** (1), 13-31.

Chu, V.H., Liu, F. and Altai, W. (2004) Friction and confinement effects on a shallow recirculating flow. *Journal of Environmental Engineering and Science*, **3**, 463-475.

Dufresne, M. (2008) La modélisation 3D du transport solide dans les bassins en assainissement : du pilote expérimental à l'ouvrage réel. [Three-dimensional modelling of sediment transport in sewer detention tanks: physical model and real-life application] PhD thesis, Université de Strasbourg (in French).
Dufresne, M., Dewals, B.J., Erpicum, S., Archambeau, P. and Pirotton, M. (2010a) Classification of flow patterns in rectangular shallow reservoirs. *Journal of Hydraulic Research*, **48** (2), 197-204.
Dufresne, M., Dewals, B.J., Erpicum, S., Archambeau, P. and Pirotton, M. (2010b) Experimental investigation of flow pattern and sediment deposition in rectangular shallow reservoirs. *International Journal of Sediment Research*, **25** (3), 258-270.
Fearn, R.M., Mullin, T. and Cliffe, K.A. (1990) Nonlinear flow phenomena in a symmetric sudden expansion. *Journal of Fluid Mechanics*, **211**, 595-608.
Garde, R.J., Ranga Raju, K.G. and Sujudi, A.W.R. (1990) Design of settling basins. *Journal of Hydraulic Research*, **28** (1), 81-91.
Giger, M., Dracos, T. and Jirka, G.H. (1991) Entrainment and mixing in plane turbulent jets in shallow water. *Journal of Hydraulic Research*, **29** (5), 615-642.
Henderson, F.M. (1966) Open channel flow. Macmillan Series in Civil Engineering, Prentice Hall, New York.
Kantoush, S.A. (2008) Experimental study on the influence of the geometry of shallow reservoirs on flow patterns and sedimentation by suspended sediments. PhD thesis, Ecole Polytechnique Fédérale de Lausanne.
Kantoush, S.A., De Cesare, G., Boillat, J.L. and Schleiss, A.J. (2008) Flow field investigation in a rectangular shallow reservoir using UVP, LSPIV and numerical modelling. *Flow Measurement and Instrumentation*, **19** (3-4), 139-144.
Kowalski, R., Reuber, J. and Köngeter, J. (1999) Investigations into and optimisation of the performance of sewage detention tanks during storm rainfall events. *Water Science and Technology*, **39** (2), 43-52.
Langhaar, H.L. (1951) Dimensional analysis and theory of models. John Wiley & Sons, New York.
Luyckx, G., Vaes, G. and Berlamont, J. (1999) Experimental investigation on the efficiency of a high side weir overflow. *Water Science and Technology*, **39** (2), 61-68.
Maurel, A., Ern, P., Zielinska, B.J.A. and Wesfreid, J.E. (1996) Experimental study of self-sustained oscillations in a confined jet. *Physical Review E*, **54** (4), 3643-3651.
Ranga Raju, K.G., Kothyari, U.C., Srivastav, S. and Saxena, M. (1999) Sediment removal efficiency of settling basins. *Journal of Irrigation and Drainage Engineering*, **125** (5), 308-314.
Saul, A.J. and Ellis, D.R. (1992) Sediment deposition in storage tanks. *Water Science and Technology*, **25** (8), 189-198.
Stovin, V.R. (1996) The prediction of sediment deposition in storage chambers base on laboratory observations and numerical simulation. PhD thesis, University of Sheffield.
Stovin, V.R. and Saul, A.J. (1996) Efficiency prediction for storage chambers using computational fluid dynamics. *Water Science and Technology*, **33** (9), 163-170.
Stovin, V.R. and Saul, A.J. (1994) Sedimentation in storage tank structures. *Water Science and Technology*, **29** (1-2), 363-372.

Number of words: 4,704